

Non-contact surface wave testing of pavements: comparing a rolling microphone array with accelerometer measurements

Henrik Bjurström^{*}, Nils Ryden^a and Björn Birgisson^b

*Department of Highway and Railway Engineering, KTH Royal Institute of Technology,
Brinellvägen 23, 100 44 Stockholm, Sweden*

(Received February 9, 2014, Revised June 2, 2014, Accepted September 6, 2014)

Abstract. Rayleigh wave velocity along a straight survey line on a concrete plate is measured in order to compare different non-destructive data acquisition techniques. Results from a rolling non-contact data acquisition system using air-coupled microphones are compared to conventional stationary accelerometer results. The results show a good match between the two acquisition techniques. Rolling measurements were found to provide a fast and reliable alternative to stationary system for stiffness determination. However, the non-contact approach is shown to be sensitive to unevenness of the measured surface. Measures to overcome this disadvantage are discussed and demonstrated using both forward and reverse rolling measurements.

Keywords: non-destructive testing; seismic testing; Lamb waves; surface waves; material characterization

1. Introduction

There is a need to develop more efficient non-destructive testing (NDT) techniques for quality assurance (QA) and quality control (QC) of material stiffness in new and existing pavement structures. NDT of concrete and asphalt pavements using seismic methods can be used for stiffness characterization through the measurement of seismic wave velocities (Nazarian *et al.* 1999). However, the use of seismic velocity measurements has been hampered by the need for full contact between sensors and the pavement as well as the stationary nature of the measurements during data acquisition. Seismic NDT of pavements is mainly based on data acquisition using accelerometers (Nazarian *et al.* 1999, Yuan *et al.* 1999, Ryden and Park 2006). However, there are problems related to the usage of accelerometers. Sufficient coupling between the accelerometer and the material surface is important. These stationary measurements are time consuming when doing large scale evaluation since data have to be collected from several points and a new setup has to be made for every new measuring position. There is a need for faster measurements that can cover larger areas. Air-coupled sensors have shown promising results of providing faster measurements (Ryden *et al.* 2008).

^{*}Corresponding author, Ph.D. Student, E-mail: henbju@kth.se

^aAdjunct Professor, E-mail: nryden@kth.se

^bProfessor, E-mail: bjornbir@kth.se

During recent years several papers have presented non-contact measurements using microphones for data acquisition. Pioneering work was performed by Luukkala *et al.* (1971) showing underwater wave transmission through a plate like structure using air-coupled transducers. Castaings and Cawley (1996) successfully showed that air-coupled transducers may be used to generate and detect Lamb waves in the field of ultrasonics by performing single-sided inspections on plates. Zhu and Popovics (2001) showed that the out-of-plane motion of a concrete structure can be detected and recorded in the audio frequency range using a directional microphone pointing toward the surface. Furthermore, they showed that air-coupled receivers can be used for imaging surface-opening cracks by studying wave attenuation (Zhu and Popovics 2005). Recent results have also demonstrated the effectiveness for air-coupled measurements in the evaluation of potential delamination of bridge decks (Kee *et al.* 2012) and characterization of cracks in concrete (Kee *et al.* 2011). Ryden *et al.* (2008) have developed a rolling data acquisition system focused on seismic velocity measurements using a multichannel microphone array mounted on a trolley. The trolley uses ordinary non-directional microphones in the audio frequency range and is operated at normal walking speed, where data are collected continuously during the rolling operation. Multichannel Analysis of Surface Waves (MASW) (Park *et al.* 1999) is used to determine the dispersion curves during rolling operation. In this study, measured Rayleigh wave velocities while rolling with the trolley (Ryden *et al.* 2008), are compared with Rayleigh wave velocity measurements using conventional stationary accelerometers. The Rayleigh wave velocity may be achieved by simply dividing the known distance between two receivers by the travel time. However, since the velocity of surface waves is in general frequency dependent (dispersive), the MASW method, based on a temporal and a spatial Fourier transform, is used in order to extract the Rayleigh wave velocity in frequency domain. The ability to measure dispersion curves while rolling over the surface can also open up future possibilities to extract velocity as a function of depth from the surface (Ryden and Park 2006). This way of comparing rolling measurements to conventional stationary accelerometer measurements using MASW has not been performed earlier.

This paper is focused on measuring the Rayleigh wave velocity in a concrete slab using a rolling multichannel non-contact microphone array. Data are collected in 60 positions while rolling along a straight line to estimate the seismic velocity (stiffness) variation along the plate. The non-contact rolling receiver array is evaluated by comparing the results to data collected with conventional accelerometers at a number of points along the tested line. Results from both methods agree well in many positions, but the rolling velocity measurements are found to be sensitive to unevenness in the concrete surface, which is discussed. The results also established a high degree of repeatability of the rolling non-contact microphone-based measurements when compared to the stationary accelerometer-based measurements.

2. Theory

Seismic waves propagating in a medium in which the wave velocity is higher than in the surrounding medium will “leak” energy into the lower velocity medium (refraction). The leakage takes place at an angle described by Snell’s law (1)

$$\alpha = \sin^{-1}\left(\frac{c_1}{c_2}\right) \quad (1)$$

where c_1 is the wave velocity in the slow medium (here air) and c_2 is the surface wave velocity in the fast medium (here concrete). The angle $\alpha = 0$ is defined as the normal to the interface. There is thus an inherent limitation that the refraction can only take place from the faster to the slower medium and not the other way around.

To measure the accurate surface wave velocity using the microphone array, it is assumed that all the microphones are perfectly aligned with the measured surface. The same distance between the material surface and each of the microphones is essential to get a correct result. This assumption may never be fully met in reality due to unevenness in the surface. An uneven surface or a tilted microphone array, like the dashed lines in Fig. 1, will cause the system to register a lower or higher apparent phase velocity. The effect of a tilted microphone array is examined in this paper.

In this study the refracted wave field comes from a homogenous concrete plate between the basement and the first floor in one of the University buildings at Lund’s University, Sweden. Guided waves bounded by two parallel surfaces in a free plate are called Lamb waves. Propagation of Lamb waves is only possible for certain combinations of frequency and phase velocity explained by Lamb’s dispersion curves, Fig. 2. There are an infinite number of dispersion curves, all divided into two families, symmetrical (S) and antisymmetrical (A) modes. The out of plane response is dominated by the fundamental antisymmetric Lamb mode (A0) when an impact normal to the surface is used (Gibson and Popovics 2005). The main target in this study is the Rayleigh wave velocity which is the asymptotic velocity of the A0 and S0 modes at high frequencies where these modes are non-dispersive (Fig. 2).

There are other good methods of estimating the Rayleigh wave velocity besides the method described. Aggelis *et al.* (2010) describe one such method where large surface deflections significant for Rayleigh waves are studied in time domain. However, working with dispersion curves in frequency domain is a robust method of estimating the Rayleigh wave velocity and enables estimation of other material parameters such as plate thickness and Poisson’s ratio in future research.

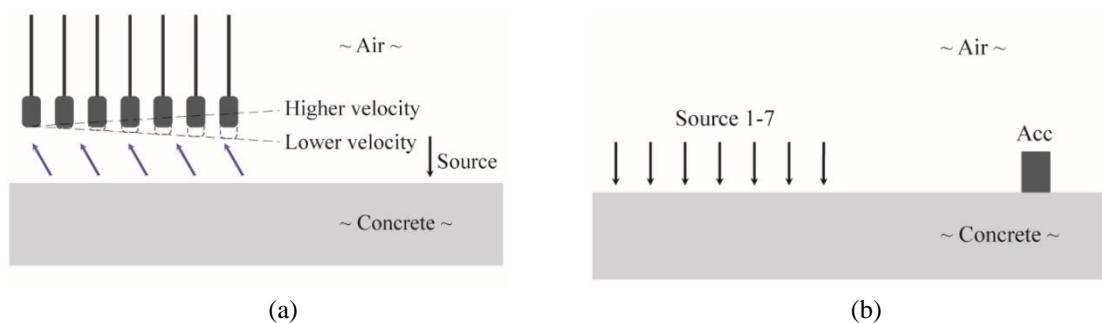


Fig. 1 Schematic sketch of the equipment setup. (a) shows the microphone array while and (b) illustrates the accelerometer approach using one receiver and multiple impact points

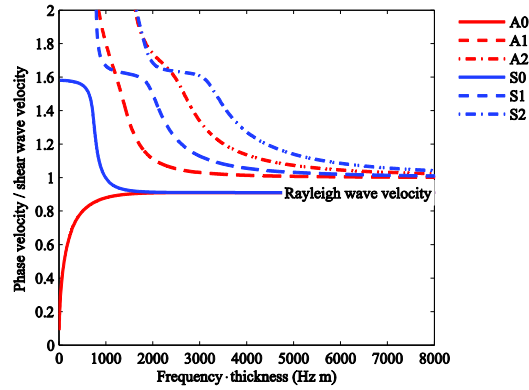


Fig. 2 Lamb's dispersion curves for a free plate with Poisson's ratio = 0.2. The curves are normalized with respect to plate thickness and shear wave velocity

3. Method

Measurements performed using air-coupled receivers are used to collect data while moving over the surface. The data acquisition process is thus made simpler than when using accelerometers since measurements may be performed for multiple positions while rolling along the surface. All the equipment needed for data acquisition and data processing are mounted on a trolley specially built for this purpose. The equipment is therefore very mobile and the entire measuring line (here 60 positions) is measured and evaluated within seconds.

Data acquisition is performed using ordinary audio microphones (ADK SC-1 condenser microphone [10 mV/Pa]) and ordinary accelerometers (PCB model 356A15 [103.3 mV/g]). The impact source is a small metal screw (~10 g) mounted on a flexible metal stick. A small piezo-ceramic element is epoxy glued on top of the screw and used to get a trigger signal for the data acquisition system. All microphones are connected to an amplifier (SM Pro Audio PR8E). Data are collected and converted from analog to digital signals using a DAQ device (DAQ NI USB 6251). The DAQ device is connected to a laptop for data processing and storage. All devices are battery powered and mounted on a trolley (Fig. 3).

To compare the measuring methods, data are first collected along a straight line using a set of microphones mounted on the trolley. An array of seven microphones is mounted with 0.05 m increments on the trolley (shown in Fig. 3) specially built for this kind of measurements by Ryden *et al.* (2008). The microphone tips are set 0.02 m above the concrete surface. The impact source is also mounted on the trolley, 0.635 m in front of and 0.085 m transverse of the first microphone, and triggered automatically by the front wheel when rolling. The source offset (0.085 m) against the exact receiver array line extension (see Fig. 3), is accounted for when calculating the distances from the source to each receiver which is used in the MASW data processing. The microphone array is 0.30 m long from the first to last microphone and the data evaluated from one measuring position is an average value of the velocity over the microphone array length. Data are collected with 0.16 m increments so there will be overlaps between the measuring array positions. The seven microphones collect data on different channels simultaneously for 5 milliseconds with a sample rate of 125 kHz. The survey line is tested five times to evaluate the repeatability.

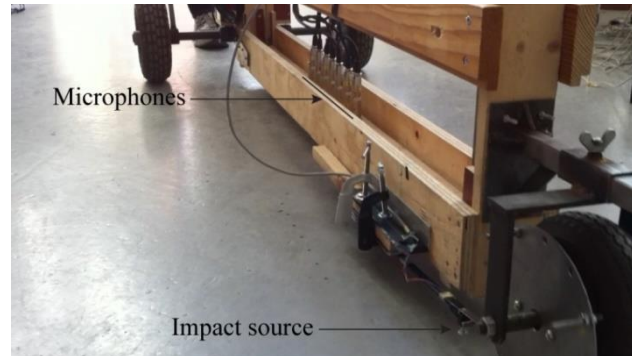


Fig. 3 All equipment is mounted on the trolley. The impact is made automatically by the front wheel when rolling

For comparison purposes data are also collected using an accelerometer attached to the concrete surface in 12 different positions with equal increments along the tested survey line. The comparison of results in this paper is limited to the asymptotic trend of the fundamental anti-symmetric (A0) Lamb wave dispersion curve at high frequencies, Rayleigh wave velocity V_R (Fig. 2). The Rayleigh wave velocity is together with Poisson's ratio directly connected to the material stiffness. A Matlab algorithm is written to automatically evaluate the Rayleigh wave velocity in every position along the measured line while rolling. Surface waves with wavelengths shorter than the plate thickness will have a constant velocity, see asymptotic part (>2500 Hzm) of the A0 mode in Fig. 2. The calculated Multichannel Analysis of Surface Waves (MASW) (Park *et al.* 1999) phase velocity spectrum is thus summed horizontally for every phase velocity over a chosen frequency spectrum and the maximum total amplitude is taken as the Rayleigh wave velocity. The procedure is performed automatically and objectively for every measuring position and a velocity variation along the survey line is plotted in the result chapter. The data collected by the accelerometers are evaluated in exactly the same way as the microphone data and also plotted in the same figures to compare the results from the two data acquisition methods.

Fig. 4 shows a sketch of the concrete floor tested. The concrete beams under the floor are marked together with cracks visible on the concrete surface.

Twelve of the measuring positions along the data collection line are tested using an accelerometer. These positions are marked with numbers in Fig. 4. The accelerometer is attached to the concrete surface using sticky grease in the point of the impact from the microphone measurement setup according to Fig. 1(a). Five impacts are averaged in each of the seven positions where the microphones were positioned during the microphone test, Fig. 1(b). Five impacts are used instead of one to increase signal to noise ratio and thereby to some degree compensate for the fact that the accelerometer measurements are used with only one accelerometer and multiple manual impacts. Despite that the data sets are collected in different ways, they are comparable due to reciprocity, a signal from a point A to a point B is equal to a signal from B to A.

To ensure that accelerometer and microphone measurements are comparable and equally affected by the subsequent data processing, the accelerometer signals are first shifted in time due to small differences in trigger and height above the surface. Before shifting the accelerometer signal, it is integrated to vibration velocity since air pressure is proportional to surface velocity.

The time signal is shifted to match the first negative peak. Response signals from one accelerometer and one microphone are plotted in time domain in Fig. 5. This time shift accounts for the differences between the two data acquisition methods. Fig. 5 shows the response from the first signal in the array at position 36 and the corresponding accelerometer signal (see plate sketch in Fig. 4). Some differences in amplitude between the two signals can be observed but they are synchronized in time. All the accelerometer signals in this study are shifted with the same constant time shift before further processing.

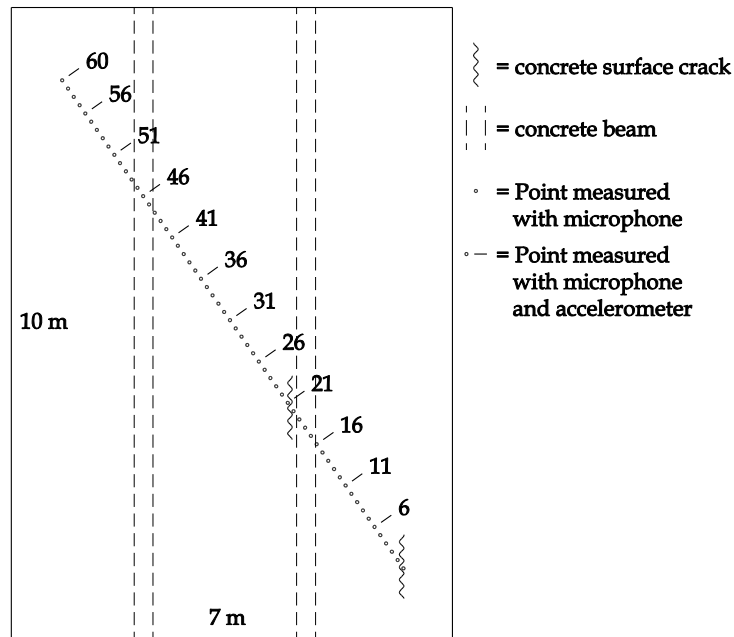


Fig. 4 Sketch of the tested concrete plate. Beams directly under the plate are marked together with visible concrete surface cracks

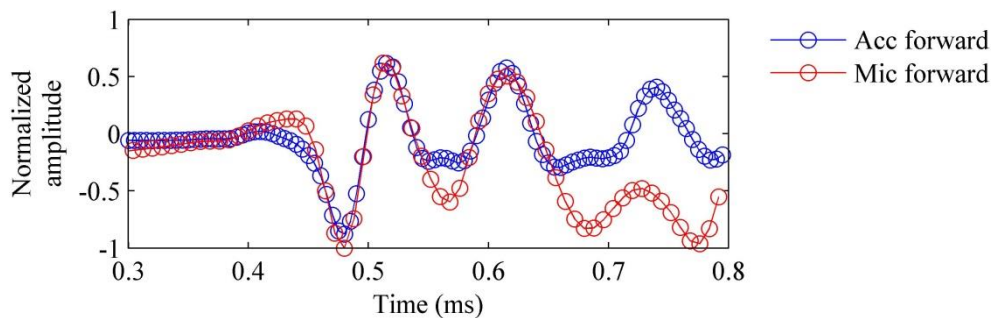


Fig. 5 Raw data from measuring position 36 plotted in time domain. The accelerometer signal is adjusted in time to match the first negative peak. The response signals are very similar regardless of the receiver type

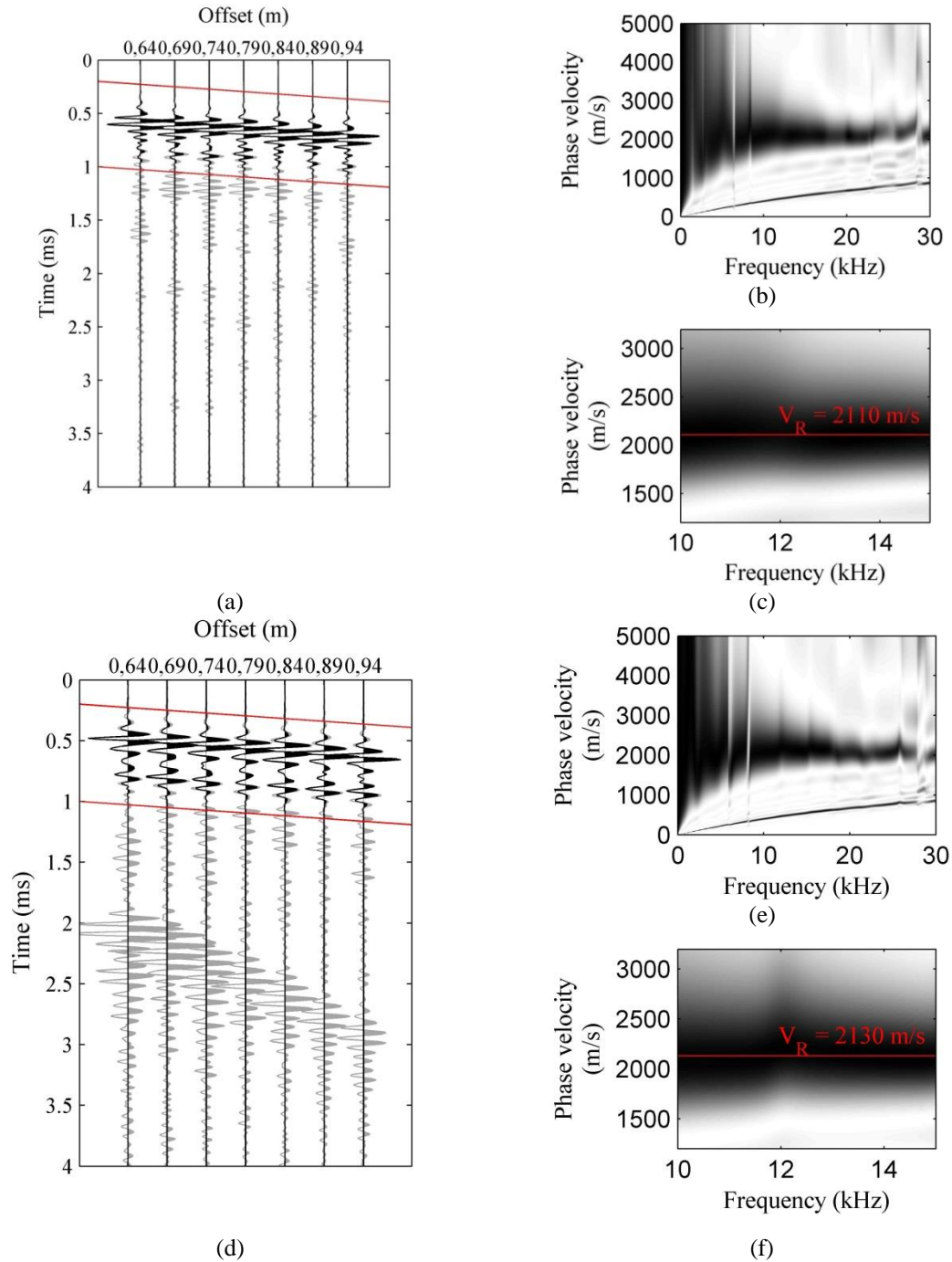


Fig. 6 Raw data for measuring positions 36 in time domain for (a) accelerometer and (d) microphone. The raw data are filtered and transformed into frequency domain using the MASW technique. The phase velocity spectrum is plotted for (b) accelerometers and (e) microphones. The frequency range used when calculating is shown in (c) and (f) for respective receiver

All recorded data sets are automatically frequency filtered and windowed in time domain before calculating phase velocities. Each data set is first high pass filtered (10 kHz) to remove low frequency noise. A cosine-tapered time window is then applied with a taper to constant value of 0.7, where 1 represents Hann window and 0 a rectangular window. The window is applied over the leaky surface wave to suppress the direct air wave and noise according to Figs. 6(a) and 6(d). The beginning and end of the time domain windows are marked with red lines in the figure. The window length is 0.8 ms and the start and end times for each channel are adjusted according to its offset from the impact point corresponding to a velocity of 2200 m/s. The unwindowed raw data are left faded (gray) in the figure. Figs. 6(a) and 6(d) show raw data collected using accelerometers and microphone respectively. The direct sound wave through the air is clearly shown as a wave package starting at ~ 2 ms with a velocity of ~ 344 m/s in Fig. 6(d).

After frequency filtering and time domain windowing, each data set is transformed to a phase velocity spectrum using the MASW technique (Figs. 6(b) and 6(e)). The Rayleigh wave velocity is estimated in a limited frequency range, 10-15 kHz, and phase velocity span, 1200-3200 m/s, see Figs. 6(c) and 6(f). These limits are set with respect to the best signal to noise ratio in both accelerometer and microphone data. Furthermore, both receiver types have a linear response in this frequency band. The microphone data show good signal to noise ratio at even higher frequencies compared to the accelerometer data. The Rayleigh wave velocity is estimated automatically by summing the amplitudes over the chosen frequency range and singling out the resulting peak phase velocity as described above. The example in Fig. 6 is taken from measuring position 36 (see Fig. 4) and the Rayleigh wave velocities are estimated to 2110 m/s and 2130 m/s respectively, see Figs. 6(c) and 6(f). These velocities are assumed to be representative of a mean velocity in the concrete over the length of the array (0.30 m). The described data processing steps are automated in a Matlab script and applied to all data sets in this study.

The main objective in this paper is to compare the measured Rayleigh wave velocity results from rolling microphone measurements and stationary measurements using one accelerometer. The measured amplitudes represent air pressure and out of plane acceleration respectively. It should be noted that the absolute amplitude or type of amplitude does not matter since it is only the relative velocity of the energy within the receiver array that is analyzed.

4. Results and discussion

All recorded individual data sets have been processed as described above and the resulting Rayleigh wave velocity over the complete survey line is analyzed. Fig. 7 shows the velocity variation along the survey line using both accelerometers and non-contact microphones as receivers. The length of the array is illustrated with horizontal markers in the trace results from the microphone data sets. As can be seen from the overlap of the microphone distance markers there is an overlap between the measurement positions thus resulting in significantly more data than the stationary accelerometer results. The results presented in Fig. 7 show that the repeatability is high. The variability from test to test is small even though as expected the variations along the line are larger (up to ca. 500 m/s). The biggest difference between a single test value and the mean from the five test values in the same measuring position is 2 %. It should be pointed out that the trolley is not pushed back and forth in the same position but the whole line is measured in one take and repeated 5 times. Fig. 7 further shows that the accelerometer measurements (black squares) correspond fairly well to the mobile microphone measurements.

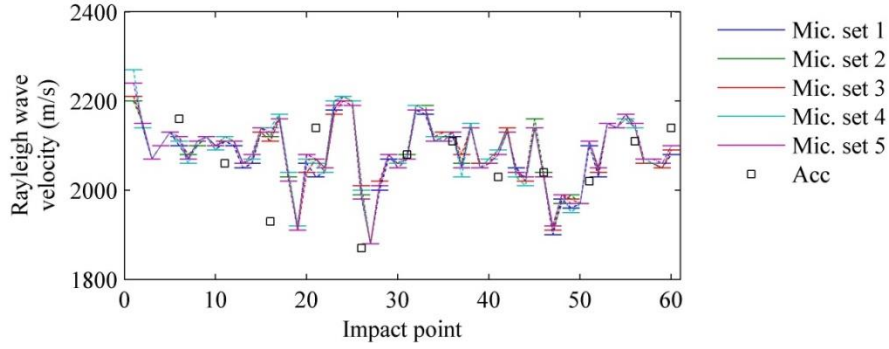


Fig. 7 Rayleigh wave velocity variation along the measuring line. Data are collected using both accelerometers and microphones. The microphone array length is shown with horizontal lines as markers

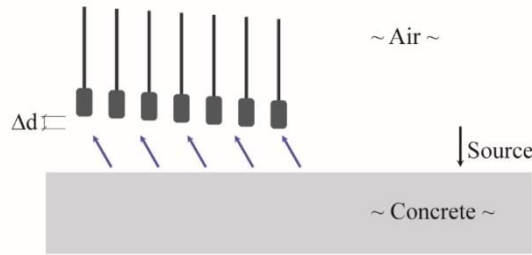


Fig. 8 A tilted microphone array or a corresponding uneven material surface will result in erroneous phase velocities

The observed velocity variations along the tested line may have several explanations. Some variation is due to the natural variations in the material but some variations may have other explanations. An unevenness of the measured surface or a tilted microphone array would affect the velocity variation significantly.

The relative velocity over the length of the array (D) can be calculated by Eq. (2)

$$v_R = \frac{D}{t} \tag{2}$$

where t is the travel time of the surface wave. Introducing an additional vertical distance Δd to the last microphone in the receiver array according to Fig. 8, representing a tilted microphone array, gives an additional travel time (Δt) in Eq. (3)

$$\Delta t = \frac{\Delta d}{v_{air} \cdot \cos\left(\sin^{-1}\left(\frac{v_{air}}{v_R}\right)\right)} \tag{3}$$

where $\sin^{-1}\left(\frac{v_{air}}{v_R}\right)$ is the leakage angle according to Snell's law.

Using trigonometry, the Δt expression is simplified to Eq. (4)

$$\Delta t = \frac{\Delta d}{v_{air} \cdot \sqrt{1 - \left(\frac{v_{air}}{v_R}\right)^2}} \quad (4)$$

The extra travel time Δt will cause the system to register a higher or lower velocity according to Fig. 1(a). The registered phase velocity becomes

$$v_{R,new} = \frac{D}{t + \Delta t} = \frac{D}{\frac{D}{v_R} + \frac{\Delta d}{v_{air} \cdot \sqrt{1 - \left(\frac{v_{air}}{v_R}\right)^2}}} \quad (5)$$

In Fig. 9 the relative error in the relevant phase velocity range when entering a small Δd is shown. It can be seen that a Δd of a few millimeters is enough to cause a major error in recorded phase velocity when using the microphone array length of 0.3 m, as in this paper, and assuming a wave velocity through air of 344 m/s. In reality some surface unevenness and roughness will always exist when measuring on materials like concrete or asphalt. It is difficult to quantify the exact unevenness along the complete survey line used in this study. However, when estimating the surface unevenness using a 4 m long straight metal bar, distances in the same range as in Fig. 9 were observed.

In order to further examine the results from the microphone measuring line, the trolley is turned around and rolled in the opposite direction along the same survey line. In this way some of the differences would be compensated (Soltani *et al.* 2013). A recorded higher velocity due to an uneven surface, or equally a tilted microphone array (see Fig. 8), measured in one direction should be able to compensate a recorded lower velocity measured in the opposite direction due to the same unevenness with the opposite sign. When rolling the trolley in the backward direction, the microphone array is located in the same position as before but with the source and microphones in the reversed order. The impact source is thus located on the other side of the microphone array. The calculated velocity is an average of the velocity over the same distance as before though. To allow for the smoothing out of the unevenness differences in the way explained above, three conditions have to be fulfilled. #1 The unevenness has to be shorter than the wheelbase of the trolley, otherwise the trolley will incline together with the surface slope (all microphones will be equally distanced from the surface) and thus give a correct velocity measurement, see Fig. 10(a). #2 The microphone array must further be placed exactly in the middle of the wheel base of the trolley to ensure that the unevenness when rolling forward and backward will be equally large. #3 The unevenness also has to be constant over the microphone array length (0.3 m) in order to not introduce non-linear errors within the arrays. Fig. 10(b) illustrates a surface where the distance between microphones and surface varies irregularly within the microphone array. This will cause errors which will not be compensated by backward rolling.

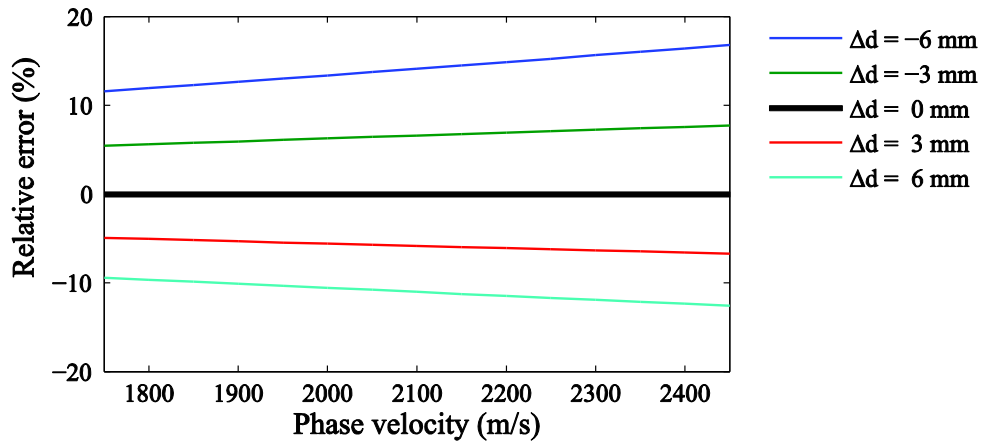


Fig. 9 Relative errors in the relevant phase velocity range for concrete. The five lines represent different values of Δd . All errors are calculated using a microphone array length of 0.3 m



Fig. 10 Schematic picture of the trolley on an unevenness (a) longer than the wheelbase of the trolley and (b) shorter than the microphone array length. The microphone array is located in the same position rolling in both directions.

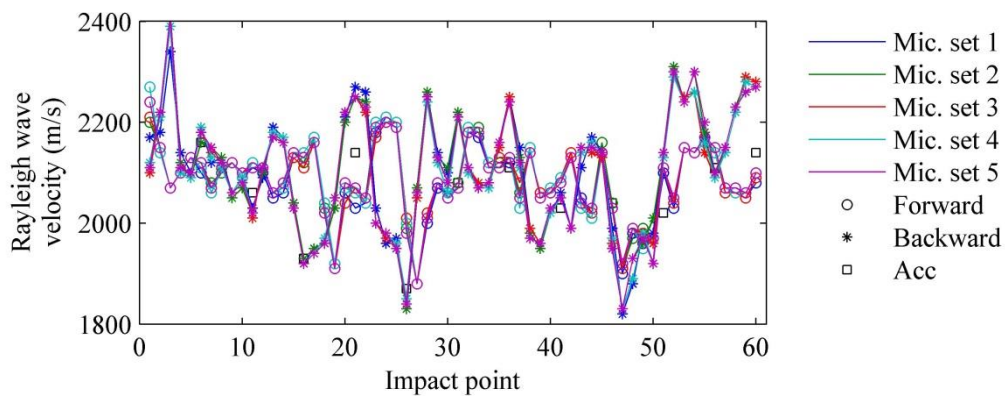


Fig. 11 Rayleigh wave velocity measured in ten sets along the survey line, five times measured in each direction

The results from the backward and forward rolling measurements are together with the accelerometer measurements shown in Fig. 11. The backward rolling measurements are also repeated along the whole line five times to ensure the repeatability. Plotting these new five lines using a synchronized x-axis reveals some differences between forward and backward measurements although the repeatability of each direction is good, see Fig. 11.

In theory and under the three conditions mentioned above, the forward and backward rolling measurements would even out which would mean that the mean value would be equal to the accelerometer measurements (independent of the surface unevenness). Measuring point 11 is an example where there is a large velocity difference between the forward and backward rolling measurements. Rolling forward gives a Rayleigh wave velocity of 2114 m/s when taking a mean of the five separate sets while rolling backward results in a corresponding velocity of 2020 m/s. The mean value from these two 2067 m/s which is very close to the 2060 m/s received from the accelerometer measurements in the same point.

The same procedure is performed for all 60 measuring positions. The result is a velocity variation containing ten different measuring sets, five measured forward and five backward. The mean value from all ten sets are calculated and plotted as a mean velocity variation line. This way the unevenness of the measured surface is partly taken into account. The mean velocity variation line is shown in Fig. 12.

To illustrate how small the variations between the different measurement sets in the same direction are, the standard deviation s , defined by

$$s = \sqrt{\frac{1}{n-1} \sum_{i=1}^n (x_i - \bar{x})^2} \quad (6)$$

is calculated, x_i being the individual measurements and \bar{x} the mean from the five measurements in each position. n is the number of measurements. The standard deviation is plotted together with mean velocity line in Fig. 12.

The standard deviation calculation is based on the data sets collected when rolling forward. The mean standard deviation is below 20 m/s, which is below 1%.

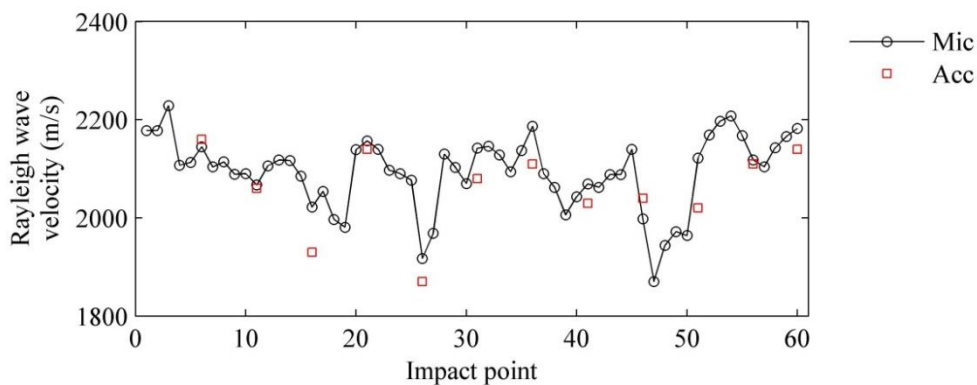


Fig. 12 Velocity variation line averaged from 10 different measuring sets, five measured forward and five backward

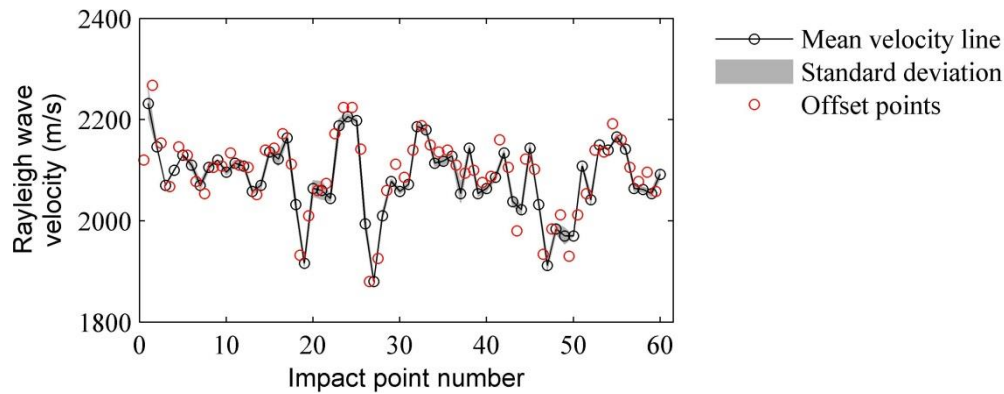


Fig. 13 Five shifted measuring sets are averaged and plotted to illustrate the reliability of the measurements. Standard deviation calculated for the five measuring sets performed by rolling forward is also shown.

To further examine the repeatability, another five measuring sets are collected in the forward direction. The data are here collected with the trolley shifted half an increment from the prior forward lines, i.e., 0.08 m. The idea is to collect data from more measuring points to investigate whether these points “fill in” the prior curves or if they make them disperse. The mean values taken from the five sets in each of the 60 measuring positions are calculated and plotted on top of the mean forward velocity line in Fig. 13. The figure shows a high repeatability in the forward rolling microphone measurements.

5. Conclusions

This paper is mainly focused on measuring the Rayleigh wave velocity in concrete plates comparing air-coupled microphone receivers to contact accelerometer receivers. In addition, the viability of a rolling microphone receiver array was assessed.

The results presented in this paper indicate:

- That nondestructive seismic testing using rolling air-coupled microphones results in similar surface wave velocities as those obtained using contact accelerometers as receivers.
- The results obtained with the rolling microphone receiver system were found to be of high repeatability.
- The unevenness of the measured surface affects the recorded velocity significantly. The microphone array and the measured surface have to be perfectly aligned to get consistent results. A small misalignment may cause the system to record a too low or too high velocity.

In summary the results presented in this paper indicate that rolling non-contact measurements enable data acquisition for large scale measuring within a fraction of the time compared to traditional stationary contact measurements. The main focus of this study has been to analyze the

mean surface wave velocity in plate like structures for the development towards more efficient future quality control of pavement material stiffness. However the same raw data can possibly also be used for other measurements such as material attenuation, detection of delaminations and crack characterization.

However, there are remaining issues with the surface evenness and roughness that still need to be overcome.

An alternative could possibly be to measure the distance from each microphone to the measured surface, e.g., ultrasonic or laser-based measurements and adjust for any differences in distance when performing the MASW. Also the number of receivers is limited to seven in this paper. A higher number of receivers would also likely result in even more robust measurement result. However, using more microphones might possibly compromise the mobility of the rolling sensor array.

Acknowledgments

The authors would like to thank the Swedish Transport Administration (Trafikverket) and the Swedish construction industry's organization for research and development (SBUF) for their financial support.

References

- Aggelis, D.G., Kordatos, E.Z., Soulioti, D.V. and Matikas, T.E. (2010), "Combined use of thermography and ultrasound for the characterization of subsurface cracks in concrete", *Constr. Build. Mater.*, **24**(10), 1888-1897.
- Castaings, M. and Cawley, P. (1996), "The generation, propagation, and detection of Lamb waves in plates using air-coupled ultrasonic transducers", *J. Acoust. Soc. Am.*, **100** (5), 3070-3077.
- Gibson, A. and Popovics, J. (2005), "Lamb wave basis for impact-echo method analysis", *J. Eng. Mech. - ASCE*, **131**(4), 438-443.
- Kee, S.H., Fernández-Gómez, E. and Zhu, J. (2011), "Evaluating surface-breaking cracks in concrete using air-coupled sensors", *ACI Mater. J.*, **108**(5), 558-565.
- Kee, S.H., Oh, T., Popovics, J.S., Arndt, R.W. and Zhu, J. (2012), "Nondestructive bridge deck testing with air-coupled impact-echo and infrared thermography", *J. Bridge Eng.*, **17**(6), 928-939.
- Luukkala, M., Heikkilä, P. and Surakka, J. (1971), "The wave resonance – a contactless test method", *Ultrasonics*, **9** (4), 201-208.
- Nazarian, S., Yuan, D. and Tandon, V. (1999), "Structural field testing of flexible pavement layers with seismic methods for quality control", *J. Transp. Res. Board*, **1654**, 50-60.
- Park, C.B., Miller, R.D. and Xia, J. (1999), "Multichannel analysis of surface waves", *Geophysics*, **64**(3), 800-808.
- Ryden, N. and Park, C.B. (2006), "Fast simulated annealing inversion of surface waves on pavements using phase velocity spectra", *Geophysics*, **71** (4), 49-58.
- Ryden, N., Lowe, M.J.S. and Cawley, P. (2008), "Non-contact surface wave scanning of pavements using a rolling microphone array", *Quantitative Nondestructive Evaluation*, Golden, Colorado, July.
- Soltani, F., Goueygou, M., Lafhaj, Z. and Piwakowski, B. (2013), "Relationship between ultrasonic Rayleigh wave propagation and capillary porosity in cement paste with variable water content", *NDT&E Int.*, **54**, 75-83.

- Zhu, J. and Popovics, J. (2001), "Non-contact detection of surface waves in concrete using an air-coupled sensor", *Quantitative Nondestructive Evaluation*, Brunswick, Maine, July.
- Zhu, J. and Popovics, J. (2005), "Non-contact imaging for surface-opening cracks in concrete with air-coupled sensors", *Mater. Struct.*, **38**(9), 801-806.
- Yuan, D., Nazarian, S., Chen, D. and McDaniel, M. (1999), "Use of seismic methods in monitoring pavement deterioration during accelerated pavement testing with TxMLS", *Proceedings of the International Conference on Accelerated Pavement Testing*, Reno, Nevada, October.

